CrossMark

RESEARCH PAPER

Combination Metabolomics Approach for Identifying Endogenous Substrates of Carnitine/Organic Cation Transporter OCTN1

Yusuke Masuo [1] • Yuri Ohba [1] • Kohei Yamada [1] • Aya Hasan Al-Shammari [1] • Natsumi Seba [1] • Noritaka Nakamichi [1] • Takuo Ogihara [2] • Munetaka Kunishima [1] • Yukio Kato [1]

ABSTRACT

Purpose Solute carrier *SLC22A4* encodes the carnitine/organic cation transporter OCTN1 and is associated with inflammatory bowel disease, although little is known about how this gene is linked to pathogenesis. The aim of the present study was to identify endogenous substrates that are associated with gastrointestinal inflammation.

Methods HEK293/OCTN1 and mock cells were incubated with colon extracts isolated from dextran sodium sulfate-induced colitis mice; the subsequent cell lysates were mixed with the amino group selective reagent 3-aminopyridyl-*N*-hydroxysuccinimidyl carbamate (APDS), to selectively label OCTN1 substrates. Precursor ion scanning against the fragment ion of APDS was then used to identify candidate OCTN1 substrates.

Results Over 10,000 peaks were detected by precursor ion scanning; m/z 342 had a higher signal in HEK293/OCTN1 compared to mock cells. This peak was detected as a divalent ion that contained four APDS-derived fragments and was identified as spermine. Spermine concentration in peripheral blood mononuclear cells from *octn1* gene knockout mice ($octn1^{-/-}$) was significantly lower than in wild-type mice. Lipopolysaccharide-induced gene expression of inflammatory cytokines in peritoneal macrophages from $octn1^{-/-}$ mice was lower than in wild-type mice.

Conclusions The combination metabolomics approach can provide a novel tool to identify endogenous substrates of OCTN1.

✉ Yukio Kato
ykato@p.kanazawa-u.ac.jp

[1] Faculty of Pharmacy, Institute of Medical, Pharmaceutical and Health Sciences, Kanazawa University, Kakuma-machi, Kanazawa 920-1192, Japan

[2] Faculty of Pharmacy, Takasaki University of Health and Welfare, Takasaki, Japan

ABBREVIATIONS

APDS	3-aminopyridyl-*N*-hydroxysuccinimidyl carbamate
CD	Crohn's disease
DSS	dextran sodium sulfate
ERGO	ergothioneine
IBD	inflammatory bowel diseases
LPS	lipopolysaccharide
PBMC	peripheral blood mononuclear cells
SNP	single nucleotide polymorphisms
TEA	tetraethylammonium

INTRODUCTION

Recent genome-wide linkage analyses indicate the association of various chronic diseases with membrane transporters [1]. Transporters are generally responsible for the selective membrane permeability of their substrate compounds, thereby contributing to homeostatic regulation. Therefore, identification of endogenous substrates for such disease-associated transporters can help our understanding of pathogenesis and therapeutics and/or diagnosis strategies for diseases, although there is no comprehensive strategy for identifying endogenous substrates of transporters. The solute carrier *SLC22A4* gene encodes the carnitine/organic cation transporter OCTN1 and is associated with various diseases including Crohn's disease (CD) [2], rheumatoid arthritis [3], autoimmune thyroid disease [4], and type 1 diabetes [5]. Of these, CD is an inflammatory bowel disease (IBD) characterized by inflammation and ulceration in the gastrointestinal tract. The etiology of CD is complex and considered to be a combination of genetic, environmental, and microbial factors. Chromosomal region 5q31 (IBD5) contains *SLC22A4* and the homolog *SLC22A5*

genes, and was identified as one of the IBD-susceptibility loci (2). The C1672T (L503F) single nucleotide polymorphism (SNP) in exon 9 of *OCTN1* is associated with CD risk (6), and meta-analysis from 15 studies showed the association between *OCTN1* SNPs and CD in Caucasians (7).

Despite this information on the genetic association between *SLC22A4* and CD, little is known about its possible involvement in disease pathogenesis. OCTN1 transports a wide variety of organic cations and zwitterionic compounds as substrates including endogenous, food-derived, and/or enterobacteria-derived compounds, such as carnitine (8), ergothioneine (ERGO) (9), hercynine (10), acetylcholine (11), and deoxycytidine (12), as well as xenobiotic compounds. Compared to the wild-type OCTN1 transporter, the L503F-OCTN1 mutant has increased transport activities of ERGO (13,14), tetraethylammonium (6,15), biguanides (16), and cytarabine (12); but decreased transport activates of carnitine (6), acetylcholine (11), and gabapentin (17). It was therefore, speculated that increased and/or decreased accumulation of certain OCTN1 substrates due to the L503F polymorphism might be associated with CD susceptibility (6). Indeed, ERGO stimulates proliferation of colorectal adenocarcinoma cell line Caco-2 (13). However, ERGO also exhibits antioxidant activity and may play a beneficial role in at least certain disease models (18).

Possible association of *OCTN1* with certain diseases has also been suggested by the up-regulation of its gene expression in inflamed organs. Although OCTN1 is ubiquitously expressed in the body (8), relatively higher gene expression of *OCTN1* was detected in peripheral blood mononuclear cells (PBMCs), CD14 positive cells (3,14) and peripheral leukocytes (9). Gene expression of *OCTN1* was also increased in mucosal biopsies from inflamed segments of CD patients compared to those from normal mucosa (14), as well as in intestinal epithelial cells of dextran sodium sulfate (DSS)-induced colitis mice compared to control mice (19). Lamina propria mononuclear cells isolated from DSS-treated mice showed higher ergothioneine uptake and protein expression of Octn1, comparted with those isolated from control mice (19). Certain inflammatory cytokines induce gene expression of *SLC22A4* in the human intestinal epithelial Caco-2 cell line (14), fibroblast-like synoviocyte MH7A cell line (20), and hepatic stellate LI90 cell line (21), further supporting the possible association of OCTN1 with inflammatory disease progression, although further identification of its endogenous substrates may help improve our understanding of the greater pathological roles of this transporter.

The purpose of the present study was to identify endogenous substrates of OCTN1 that are associated with IBD susceptibility. Untargeted metabolome analysis would be the most useful tool for such a purpose, but can also lead to nonspecific identification of unrelated compounds; therefore, we attempted to improve the traditional metabolomic approach by combining the following two

processes: first, extracts of inflamed intestinal tissue were used as a source for OCTN1 substrates because the expression level of *OCTN1* gene product is induced in the colon during gastrointestinal inflammation (14,19), which could concentrate disease-associated compounds in these tissues. Moreover, cultured cell lines exogenously transfected with the *OCTN1* gene (HEK293/OCTN1 cells) were exposed to the inflamed intestinal tissue extracts and used to further concentrate OCTN1 substrates into the cells by the uptake activity of the transporter in HEK293/OCTN1 cells (Fig. 1). Second, amino group-selective derivatization using 3-aminopyridyl-*N*-hydroxysuccinimidyl carbamate (APDS) of the extract of HEK293/OCTN1 cells was performed to specifically label SLC22A4 substrates (Fig. 1), since most of the OCTN1 substrates contain amino groups in their structures. Precursor ion scanning against APDS fragment ions was then performed to identify the APDS-labeled compounds. The combination of these two strategies aimed to selectively identify OCTN1 substrates that are included in inflamed intestinal tissues and potentially exclude false-positive compounds. With this combination metabolomics approach, spermine was identified as an endogenous substrate for OCTN1 in the present study. Spermine concentration in PBMCs from *octn1*$^{-/-}$ mice was lower than that in wild-type mice, suggesting possible involvement of OCTN1 in spermine homeostasis.
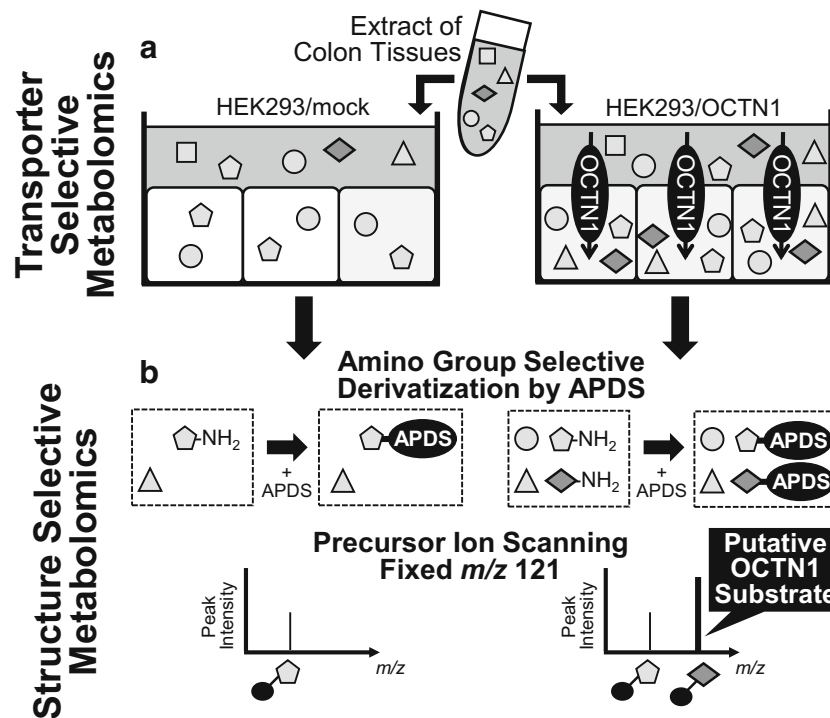
MATERIALS AND METHODS

Reagents

DSS (36,000–50,000 Da) was purchased from MP Bio Medicals (Santa Ana, CA). [^{3}H]Spermine (45 Ci/mmol) was obtained from American Radiolabeled Chemicals (Saint Louis, MO). [^{14}C]Tetraethylammonium (TEA, 45 Ci/mmol) was obtained from PerkinElmer (Waltham, MA). ERGO and ERGO-d9 were kindly provided by Dr. Jean-Claude Yadan from TETRAHEDRON (Paris, France). APDS was synthesized from *N,N'*-dihydroxysuccinimidyl carbonate (Tokyo Chemical Industry, Tokyo, Japan) and 3-aminopyridine (Sigma Aldrich, St. Louis, MO) as described previously (22), and was identified by ^{1}H-NMR. All other reagents were commercial products of reagent grade.

Animals

The *octn1*$^{-/-}$ mice were generated and backcrossed into a C57BL/6 J background (23,24). Wild-type (C57BL/6 J) and *octn1*$^{-/-}$ mice were maintained with free access to food and water. Experiments were performed according to the Guideline for the Care and Use of Laboratory Animals at

Fig. 1 **Schematic of the combination metabolomics approach for identifying endogenous OCTN1 substrates in inflamed colon tissues**. (**a**) HEK293 cells stably transfected with OCTN1 or vector alone (mock) constructs were incubated with culture medium that contained extracts of colon tissues obtained from mice with gastrointestinal inflammation or normal condition. Potential OCTN1 substrates in the biological samples were taken up and concentrated in HEK293/OCTN1 cells compared to the mock cells. (**b**) Lysates of HEK293/OCTN1 and mock cells were reacted with APDS, amino group derivatization reagent, to selectively label OCTN1 substrates, since OCTN1 preferably recognizes amino-group containing cationic compounds as its substrates. Precursor ion scanning for APDS fragment ions was performed to selectively detect APDS-derivatized compounds. Peaks with higher intensities in HEK293/OCTN1 than in mock cells were selected as candidate of OCTN1 substrates.

Kanazawa University. All protocols were approved by the Institutional Animal Care and Use Committee of Kanazawa University (approval number: AP-132875).

Preparation of Colon Extracts from DSS-Induced Colitis Mice

Experimental DSS-induced colitis was produced in mice as previously reported with minor modifications (19). Briefly, male C57BL/6 J mice (wild-type) were permitted free access to drinking water containing 2% (*w/v*) DSS from day 1 to 8, and DSS-free water from day 8 to 11. On day 11, mice were euthanized for colon tissue collection. Colon tissues were homogenized in ice-cold methanol (3 volumes by tissue weight) with 1.2 mm zirconia/silica beads (Biomedical Science, Tokyo, Japan) in a Precellys 24 homogenizer (Bertin Technologies, Montigny-le-Bretonneux, France). Homogenates were then mixed with water (1/2 volume) and chloroform (same volume), and centrifuged at 25,000 x *g* for 15 min at 4°C to remove lipids and proteins. Water/methanol layers were evaporated, resuspended in culture medium (Dulbecco's modified Eagle's medium containing 10% fetal bovine serum), and used as extract of colon tissues in uptake experiments in HEK293/OCTN1 and mock cells.

Uptake Experiments in HEK293/OCTN1 Cells Using Colon Tissue Extracts

HEK293/OCTN1 and mock cells were seeded on poly-L-lysine-coated 100 mm dishes at a density of 1.4×10^5 cells/cm². After 3 d of culture, the medium was replaced with colon tissue extracts obtained from DSS-treated mice, and incubated in a humidified incubator at 37°C with 5% CO_2 for 12 h. The medium was then aspirated, and the cells were washed twice with ice-cold PBS. Additional ice-cold PBS was applied, and cells were scraped and centrifuged at 200 x *g* for 10 min. Cell pellets were mixed with 50% MeOH and centrifuged at 25,000 x *g* for 10 min at 4°C to precipitate proteins. The supernatants were then evaporated, and the residues were dissolved in 200 µL acetonitrile: water (50: 50 *v*/v) and subjected to derivatization using APDS as a sample solution.

APDS Derivatization of Amino Group-Containing Compounds

Derivatization reactions were performed as previously reported with minor modifications (22). Briefly, a 20 µL aliquot of the reconstituted cell lysate solution was mixed with 60 µL 0.2 M sodium borate buffer (pH 8.8), and 20 µL 30 mM APDS solution dissolved in acetonitrile. The mixture was then incubated at

55°C for 60 min, followed by addition of 10 µL 60 mM aspartic acid solution and subsequent incubation for further 60 min to react with any excess APDS. Ninety microliters 0.1% (v/v) formic acid solution was then added to neutralize the solution. The obtained derivatized samples were then subjected to precursor ion scanning and single reaction monitoring using high-performance liquid chromatography-tandem quadrupole mass spectrometry (LC-TQMS), and accurate mass scanning using liquid chromatography-quadrupole time-of-flight mass spectrometry (LC-QTOFMS).

Precursor Ion Scanning Using LC-TQMS

The APDS-derivatized samples were analyzed by precursor ion scanning in a triple quadrupole mass spectrometry with a Nexera X2 LC system coupled with LCMS-8040 (Shimadzu, Kyoto, Japan). After collision-induced dissociation, APDS-tagged samples produced a common product ion, m/z 121, which represents the amino pyridine moiety [22]. Therefore, the scanning of precursor ions was performed at m/z of 150 to 500, and product ions were fixed at m/z 121. The mobile phases were (A) water containing 10 mM ammonium formate and (B) methanol containing 10 mM ammonium formate. Gradient elution (flow rate, 0.4 mL/min) was carried out as follows: 0 to 1 min, 99% A/ 1% B; 1 to 7.0 min, 99% A/ 1% B to 5% A/ 95% B; 7.0 to 8.0 min, 5% A/ 95% B; 8.0 to 8.1 min, 5% A/ 95% B to 99% A/ 1% B, on a Inertsil C8–3 column (2 µm, 2.1 × 75 mm; GL Science, Tokyo, Japan). Chromatographic and spectral data were deconvoluted using Mass++ software to construct the multivariate data matrix [25]. Cellular protein content was determined with a protein assay kit (Bio-Rad Laboratories, Hercules, CA), and the intensity of each ion was normalized by the amount of cellular protein.

Accurate Mass Scanning Using LC-QTOFMS

The APDS-derivatized samples were analyzed by accurate parent and product ion scanning with time of flight mass spectrometry on an Acquity UPLC system coupled with Xevo G2 QTOFMS (Waters, Milford, MA). For MS scanning, data were acquired in centroid mode at m/z of 50 to 800, and the collision energy was elevated from 0 to 30 V. The accurate masses of parent and product ions observed were then compared with the online METLIN database (https://metlin.scripps.edu).

Measurement of Spermine Concentration in Blood and Tissue Samples Using LC-TQMS

Mice were fasted overnight with free access to water before euthanasia, and subsequent collection of blood and tissue samples. PBMCs were isolated from blood by density gradient centrifugation according to the standard OptiPrep procedure (Alere Technologies AS, Oslo, Norway). Plasma and blood samples were mixed with three volumes of ice-cold methanol, and tissue samples were homogenized as described above. These samples were then centrifuged at 25,000 x g for 10 min at 4°C to precipitate proteins; the supernatants were collected, evaporated, dissolved in 200 µL acetonitrile: water (50: 50 v/v), and derivatized with APDS as described above. Determination of spermine concentrations was performed by LC-TQMS with a Nexera X2 LC system coupled with an LCMS-8040. The single reaction monitoring transitions of the molecular and product ions were as follows: derivatized spermine, $m/z = 342.1 > 121.0$; and derivatized gabapentin (internal standard), $m/z = 292.1 > 121.0$. For determination of spermine concentrations, the mobile phases were (A) water containing 10 mM ammonium formate and (B) methanol containing 10 mM ammonium formate. Gradient elution (flow rate, 0.4 mL/min) was carried out as follows: 0 to 1 min, 99% A/ 1% B; 1 to 4.0 min, 99% A/ 1% B to 5% A/ 95% B; 4.0 to 5.0 min, 5% A/ 95% B; 5.0 to 5.1 min, 5% A/ 95% B to 99% A/ 1% B, on a Inertsil C8–3 column (2 µm, 2.1 × 75 mm; GL Science).

Transport of [³H]Spermine, ERGO-d9, and [¹⁴C]TEA in HEK293/OCTN1 Cells

HEK293/OCTN1, HEK293/L503F-OCTN1, and mock cells were seeded onto poly-L-lysine-coated 6-well plates at a density of 1.4×10^5 cells/cm². After 3 d of culture, the medium was replaced with fresh media containing [³H]spermine, ERGO-d9, or [¹⁴C]TEA to initiate the transport. At designated times, medium was aspirated and cells were washed twice with ice-cold PBS. For the analysis of [³H]spermine transport, cells were scraped from the plates after the addition of ice-cold PBS and centrifuged at 10,000 x g for 1 min. The supernatant was removed, and cell pellets were solubilized in 0.2 N NaOH. For the analysis of [¹⁴C]TEA transport, cells were washed three times with ice-cold PBS and solubilized in 0.2 N NaOH. After neutralization with 0.2 N HCl, the radioactivity in the cell lysates and media were measured using a liquid scintillation counter (LSC-5100; Aloka, Tokyo, Japan) with Clearsol I (Nacalai Tesque, Kyoto, Japan) as the scintillation fluid. To determine uptake of ERGO-d9, cells were washed three times with ice-cold PBS and permeabilized with distilled water. The amount of ERGO-d9 in cell lysates and media was measured by LC-MS/MS as described previously [24]. Uptake of [³H]spermine, ERGO-d9, and [¹⁴C]TEA was normalized by both cellular protein amount and concentration in the medium, and represented as a distribution volume (µL/mg protein).

Isolation of Peritoneal Macrophages and Determination of mRNA Expression

Peritoneal macrophages were isolated from mice treated with thioglycolate medium (Becton, Dickinson and Company,

Sparks, MD) as previously described (26). Cells were plated at a density of 2.78×10^5 cells/cm^2 in 6-well plates and allowed to attach for 24 h. The primary cell cultures were then exposed to either 0 or 100 ng/mL lipopolysaccharide (LPS; Wako, Osaka, Japan). Total RNA was extracted according to the standard RNAiso Plus procedure (Takara Bio, Shiga, Japan). The cDNA was synthesized using an oligo $(dT)_{12–18}$ primer, deoxynucleotide triphosphate mix, RT buffer, and MultiScribe Reverse Transcriptase (Thermo Fisher Scientific, Waltham, MA); and amplified in an Mx3005P (Agilent Technologies, Santa Clara, CA) in a reaction mixture containing a cDNA template, relevant sense and antisense primers, and THUNDERBIRD SYBR qPCR Mix (TOYOBO, Osaka, Japan). The sequences of the primers were as follows: *Tnf-α* forward, CGTCGTAGCAAACCACCAAG and reverse, GAGAACCTGGGAGTAGACAAG; *Ifn-γ* forward, CACGGCACAGTCATTGAAAG and reverse, CATCCTTTTGCCAGTTCCTC; *Il-1β* forward, GCTGAAAGCTCTCCACCTCA and reverse, AGGCCACAGGTATTTTGTCG; *IL-6* forward, CCGGAGAGGAGACTTCACAG and reverse, CAGAATTGCCATTGCACAAC; *Gapdh* forward, AACTTTGGCATTGTGGAAGG and reverse, GGATGCAGGGATGATGTTCT. The PCR conditions were as follows: initial denaturation at 95°C for 15 min, followed by 40 cycles of denaturation at 95°C for 10 s and combined annealing extension at 60°C for 30 s. The expression levels of mRNA were normalized to the *Gapdh* housekeeping gene.

Statistical Analysis

All values are presented as the mean ± SEM. The statistical significance was determined by the Student's t test or, one- or two-way ANOVA with Tukey's multiple comparison test; $p < 0.05$ was considered a significant difference.
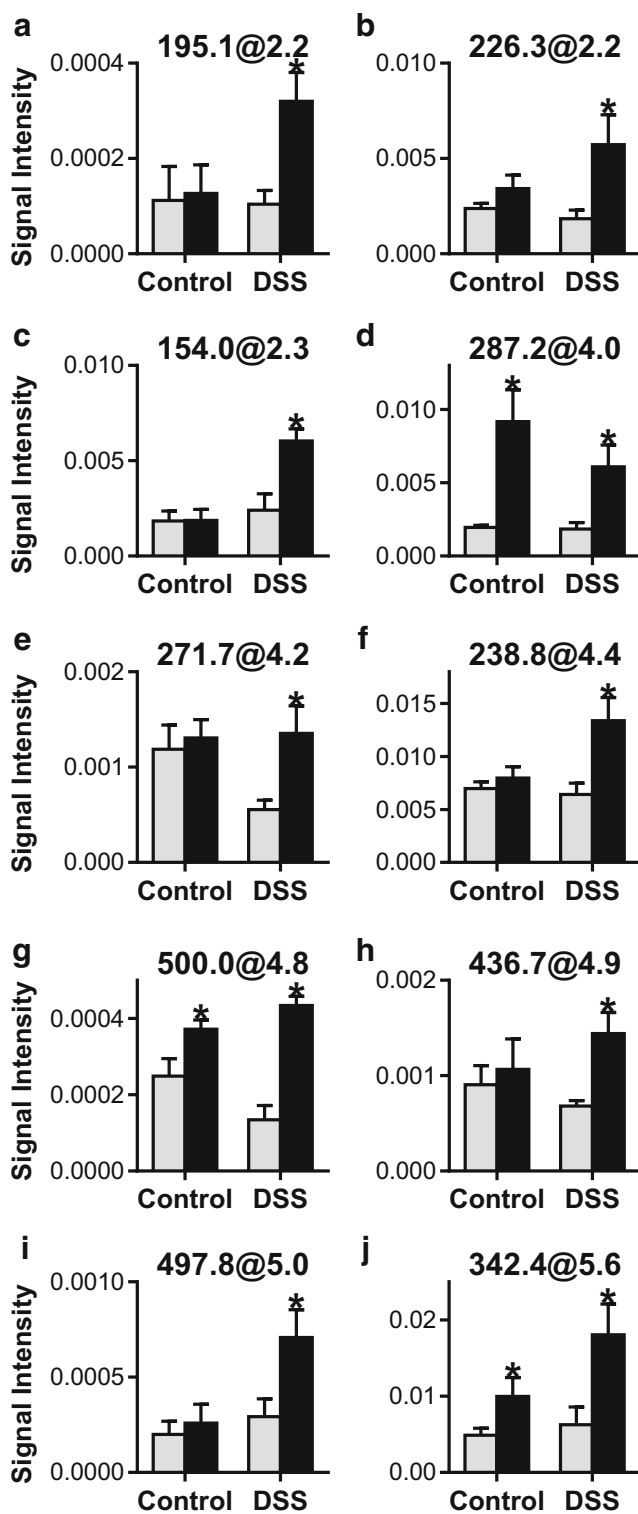
RESULTS

Combination Metabolomics Approach for Selective Identification of Endogenous OCTN1 Substrates

The combination metabolomics approach was performed to selectively identify candidate endogenous OCTN1 substrates that might be associated with gastrointestinal inflammation (Fig. 1). The first step (transporter-selective metabolomics) included the incubation of HEK293/OCTN1 or mock cells in culture medium that contained colon tissue extracts isolated from DSS-treated or control mice to concentrate potential OCTN1 substrates from the colon samples in the HEK293/OCTN1 cells (Fig. 1a). The second step (structure-selective metabolomics) included a reaction between the cell lysates and APDS, which is an amino group derivatization reagent

(22), to selectively label OCTN1 substrates, most of which contain amino groups in their structure (Fig. 1b). Precursor ion scanning against the APDS fragment ion ($C_6H_5N_2O^+$; $m/z = 121.040$; (22)) was then performed to comprehensively detect the derivatized compounds (Fig. 1b). Peaks that were higher in HEK293/OCTN1 than mock cells were selected as candidate OCTN1 substrates. After precursor ion scanning, 7538 ion peaks were detected by the automatic detection in HEK293/OCTN1 or mock cell samples. Among these, 126 peaks had significantly higher signal intensities in HEK293/OCTN1 cells compared to the mock cell samples ($p < 0.05$, fold increase >2). Among these peaks, 12 had sufficient signals with signal-to-noise ratios >5; furthermore, 10 peaks had significantly higher signal intensities in HEK293/OCTN1 cells compared to the mock cells (Fig. 2). Three peaks at m/z 287.2, 500.0, and 342.4 showed significantly higher signal intensities in HEK293/OCTN1 cells when either DSS-treated or control mouse colon samples were used (Fig. 2). Significantly higher signal intensities in HEK293/OCTN1 cells was observed for several peaks only in DSS-treated mice (Fig. 2a-c, e, f, h, i), and these may also be associated with inflammation.

Identification of Spermine as a Putative OCTN1 Substrate

To identify the structure of m/z 342, which showed relatively higher signal intensities (Fig. 2j), accurate mass of parent and product ions were obtained by LC-QTOFMS. The accurate mass was detected as 342.181 at retention time of 6.0 min (Fig. 3a, b). If the ion contains one ^{13}C stable isotope, a monovalent ion should be detected with $\Delta = +1.003$; nevertheless, the isotope ion for m/z 342.181 was detected at 342.683 ($\Delta = +0.501$) (Fig. 3b). Thus, m/z 342.181 was presumed to be a divalent ion. The monovalent ion of m/z 342.181 was estimated to be 683.373, and this monovalent ion (m/z 683.373) was detected at the same retention time with m/z 342.181 (Fig. 3a, b). The product ions of m/z 683.373 were next detected at m/z 563.341 ($\Delta = -120.032$), 443.299 ($\Delta = -240.074$), 323.259 ($\Delta = -360.114$), and 203.222 ~ 203.225 ($\Delta = -480.151$ or -480.148) with increasing collision energy (Fig. 3c), indicating almost an equal interval of m/z among the product ions ($\Delta\Delta = -120.0$). Since the estimated neutral loss of the APDS fragment was 120.032 ($C_6H_4N_2O$), these four product ions were presumed to be 1, 2, 3, and 4 APDS fragment(s) that were lost from the parent ion (m/z 683.3734), respectively. Therefore, m/z 683.3734 could contain four APDS fragments, indicating that before derivatization, the compound contained four amino groups and thus, the m/z for the parent compound was estimated to be 203.225. Three product ions (m/z 84.072, 112.106, and 129.134) were also detected (Fig. 3c), and these product ions were most likely derived from the parent compound, but not the APDS fragment.
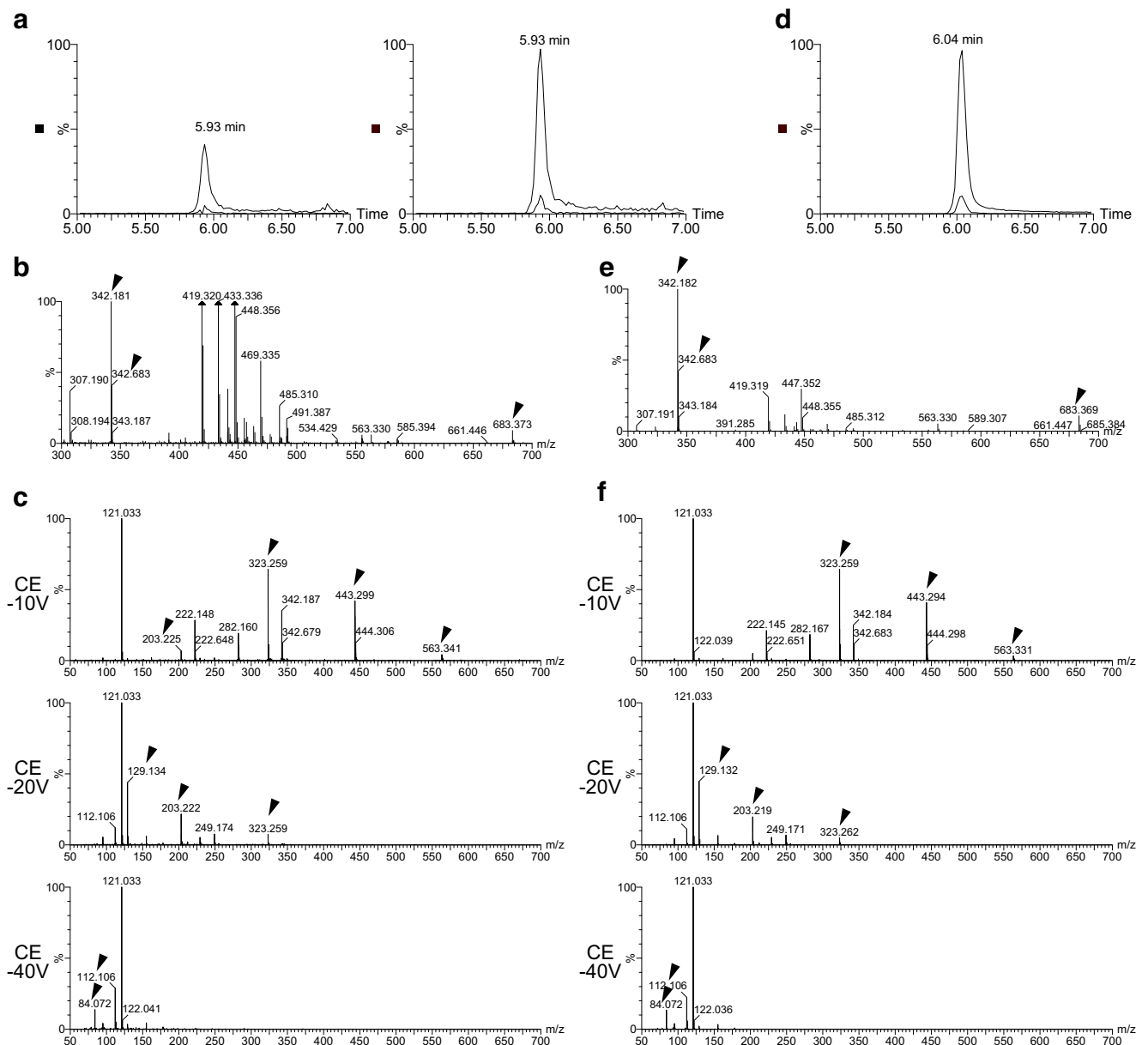
Fig. 2 Candidate endogenous OCTN1 substrates. HEK293/OCTN1 and mock cells were incubated for 12 h in culture medium containing extracts from colon tissues isolated from DSS-induced colitis or control mice. Lysates from HEK293/OCTN1 and mock were then mixed with APDS, and precursor ion scanning was performed to detect product ions (m/z 121) that were derived from the APDS fragment. Intensities of detected ions were comprehensively analyzed and ions with a higher intensity in HEK293/OCTN1 cells (black bars), compared with mock cells (gray bars), are presented. Each point represents the mean ± S.E.M. (n = 5). *: $p < 0.05$ compared with mock.

To identify the parent compound, an online metabolite database was searched for candidates that met the following conditions: (i) the parent m/z was 203.222–203.225; (ii) three product ions with m/z 84.072, 112.106, and 129.134 were released; and (iii) contained four amino groups. Spermine was finally identified as a candidate parent compound for m/z 683.373. Authentic spermine was next derivatized with APDS, and a similar chromatogram and MS(/MS) spectrum of m/z 683 were obtained between the authentic spermine and derivatized lysates from HEK293/OCTN1 cells (Fig. 3). The theoretical monovalent ion of spermine after complete derivatization by APDS is 683.353, and the difference between the theoretical and observed mass was quite small, less than 50 ppm (Table I). The theoretical mass of the product ions of the derivatized spermine (m/z 563.321, 443.288, and 323.256) was also quite similar to the observed mass of the product ions (Table I). Therefore, spermine was identified as a putative OCTN1 substrate in DSS-treated mouse colons.

Interaction between Spermine and OCTN1

Uptake of [³H]spermine in HEK293/OCTN1 and mock cells was examined to identify a possible interaction between spermine and OCTN1. Since L503F-OCTN1 was reported to have higher transport activity of various substrates (6,12–16) and increase the risk of Crohn's disease (6,7), [³H]spermine uptake in HEK293/L503F-OCTN1 cells was also examined. [³H]Spermine exhibited extensive adsorption to the surface of culture dishes, and its uptake could not be determined when the incubation was performed in the absence of proteins. Therefore, the uptake study was performed using medium that included 10% FBS. Under these conditions, the uptake of [³H]spermine in HEK293/L503F-OCTN1 cells gradually increased over time and was higher than in mock cells, although high background uptake of [³H]spermine was observed in mock cells (Fig. 4a). By comparing the uptake at 1 and 6 h, the mean value for the slope was estimated to be 248 and 126 μL/mg protein/5 h in HEK293/L503F-OCTN1 and mock cells, respectively, the former being higher than the latter (Fig. 4a). Nevertheless, the uptake profile in these cell lines may also provide the difference in y-intercept between each cell line (Fig. 4a), implying that binding and/or other mechanism than the cellular uptake may also be involved. Uptake of [³H]spermine in HEK293/OCTN1 cells tended to be slightly higher than that in mock cells (Fig. 4a). We next examined [³H]spermine uptake at various concentrations. Uptake of [³H]spermine in HEK293/L503F-OCTN1 cells was higher than that in mock cells at most of the evaluated spermine concentrations; and the uptake of [³H]spermine became saturated as the spermine concentration increased in all cell lines (Fig. 4b). Thus, OCTN1, especially the L503F variant, may interact with spermine, which was consistent with previous findings that
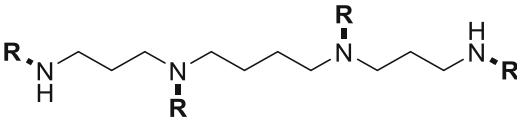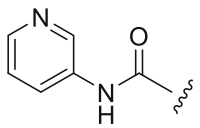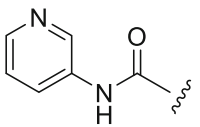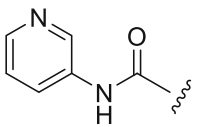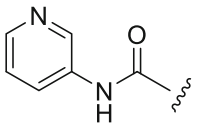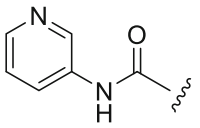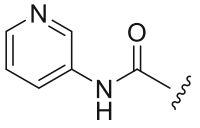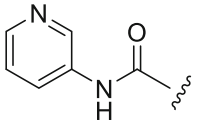
Fig. 3 Identification of spermine as a putative endogenous substrate of OCTN1. (a - c) Lysates from HEK293/OCTN1 cells that were incubated with extracts of colon tissues from DSS-induced colitis mice, and (**d** - **f**) standard solutions of authentic spermine were analyzed by LC-QTOFMS after reaction with APDS. (**a**, **b**) Parent mass scanning was performed to obtain the accurate mass of the parent compound with an ion *m/z* 342. (**a**, **d**) Representative mass chromatograms of both 342.18 (solid line) and 683.37 (dotted line) are presented. Accurate mass spectra at 6.0 min are shown in panels B and D. (**c**, **f**) Product ion scanning against *m/z* 342.2 was also performed with various collision energy between − 10 V and − 40 V.

spermine could inhibit OCTN1-mediated acetylcholine up-take in OCTN1-reconstituted liposomes (11). The inhibitory effect of verapamil on [³H]spermine uptake was examined to support the uptake of spermine into the cells. In the presence of verapamil, the uptake of [³H]spermine in HEK293/L503F-OCTN1 cells was reduced to the same level in mock cells. Similar inhibition by verapamil was also observed for the uptake of [¹⁴C]TEA (Fig. 4d), and this was consistent with the previous report that 1 mM verapamil reduced 90% of [¹⁴C]TEA uptake in HEK293/WT-OCTN1 cells (27). It should be noted that verapamil also reduced uptake of

[³H]spermine in mock cells (Fig. 4c), suggesting that spermine is transported by endogenous mechanism in HEK293 cells. The effect of spermine on typical OCTN1 substrate (e.g. ERGO and TEA) uptake was also examined to further confirm the interaction of spermine with OCTN1. High concentrations of spermine partially reduced L503F-OCTN1-mediated uptake of ERGO and TEA (Fig. 4e, f). The weak inhibition provoked by spermine was similar to the previous report that 5 mM spermine did not inhibit OCTN1-mediated TEA uptake in HEK293/OCTN1 cells (27). The effect of ERGO on the [³H]spermine uptake was also examined in

Table I   Molecular Formulas and Chemical Structures of Parent and Product Ions of APDS-Derivatized Spermine

Formula	Structure	z	Theoretical	Observed	Δppm
$C_{34}H_{42}N_{12}O_4$ Spermine + 4 × APDS	R = (pyridyl-amide) × 4	1	683.353	683.369 - 683.373	+23 +29
		2	342.180	342.181 - 342.182	+3 +6
$C_{28}H_{38}N_{10}O_3$ Spermine + 3 × APDS	R = (pyridyl-amide) × 3, H × 1	1	563.321	563.331 - 563.341	+18 +36
$C_{22}H_{34}N_8O_2$ Spermine + 2 × APDS	R = (pyridyl-amide) × 2, H × 2	1	443.288	443.294 - 443.299	+14 +25
$C_{16}H_{30}N_6O$ Spermine + 1 × APDS	R = (pyridyl-amide) × 1, H × 3	1	323.256	323.259 - 323.262	+9 +19
$C_{10}H_{26}N_4$ Spermine	R = H × 4	1	203.223	203.219 - 203.225	-20 +10

HEK293/L503F-OCTN1, HEK293/OCTN1, and mock cells, but was not significantly changed in the presence of 1 mM ERGO (data not shown).
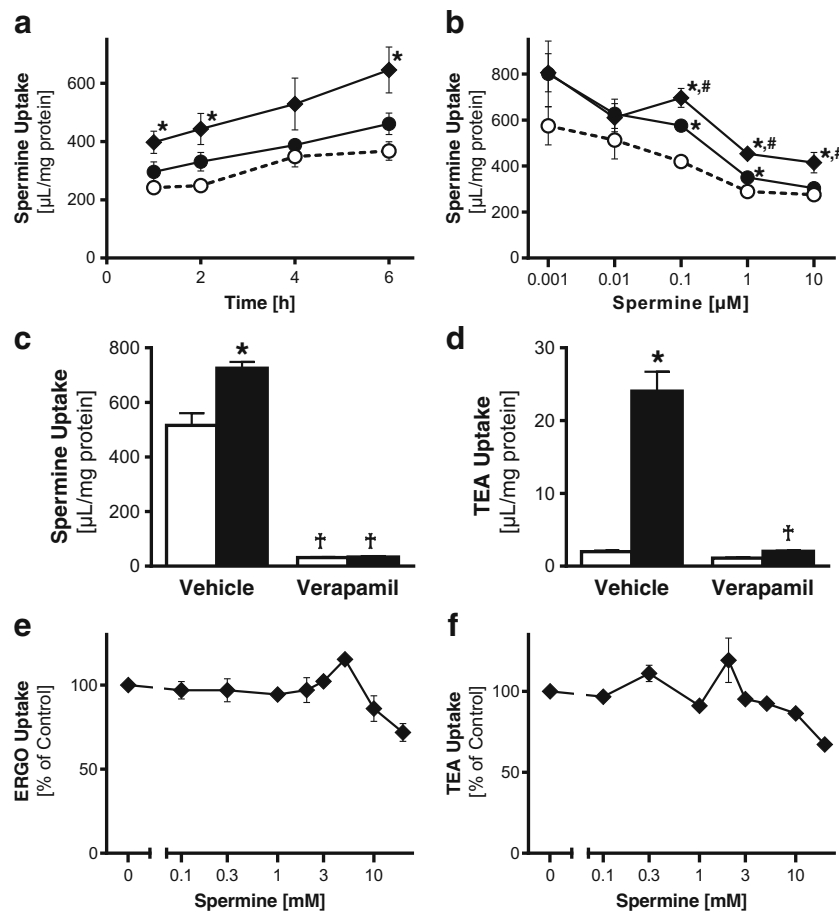
OCTN1 Regulates Spermine Concentration in PBMCs

To investigate the possible involvement of OCTN1 in spermine homeostasis *in vivo*, spermine concentrations in plasma and other organs were next measured and compared between wild type and $octn1^{-/-}$ mice. Spermine could be detected in plasma, whole blood, brain, liver, kidney, and heart in both strains, but the effect of $octn1$ gene deletion on the spermine concentration was minimally observed (Fig. 5a, b). Since OCTN1 is expressed in intestines and up-regulated during intestinal inflammation in humans [14] and mice [19], spermine concentration was measured in the mucosa of the small intestine and colon isolated from DSS-treated and control mice; however, the levels were similar between wild-type and $octn1^{-/-}$ mice (Fig. 5c). Spermine concentration was also measured in PBMCs because OCTN1 is highly expressed in CD14 positive cells [3,14], and PMBCs contain CD14 positive fractions. Spermine concentration in PBMCs isolated from $octn1^{-/-}$ mice was significantly lower than that in wild-type mice (Fig. 5d); thus, OCTN1 could contribute to the regulation of spermine concentration in PBMCs.

Effect of *octn1* Gene Deletion on LPS-Induced Inflammation in Peritoneal Macrophages

The association of OCTN1 with spermine concentration in PBMCs (Fig. 5d) led us to examine its potential role in inflammatory cells like macrophages, since spermine has an antioxidant activity, whereas one of its metabolites, acrolein, is a toxic aldehyde that increases inflammatory cytokines [28]. To identify the effect of $octn1$ gene deletion on inflammation, inflammatory responses in primary cultured peritoneal macrophages isolated from wild type and $octn1^{-/-}$ mice were examined. The mRNA expression of inflammatory cytokine genes (*TNF-α, IFN-γ, IL-1β,* and *IL-6*) in the peritoneal macrophages from both mouse strains was increased with LPS treatment (Fig. 6a-d). After the addition of LPS, the mRNA levels of *TNF-α* and *IFN-γ* in $octn1^{-/-}$ mice were significantly lower
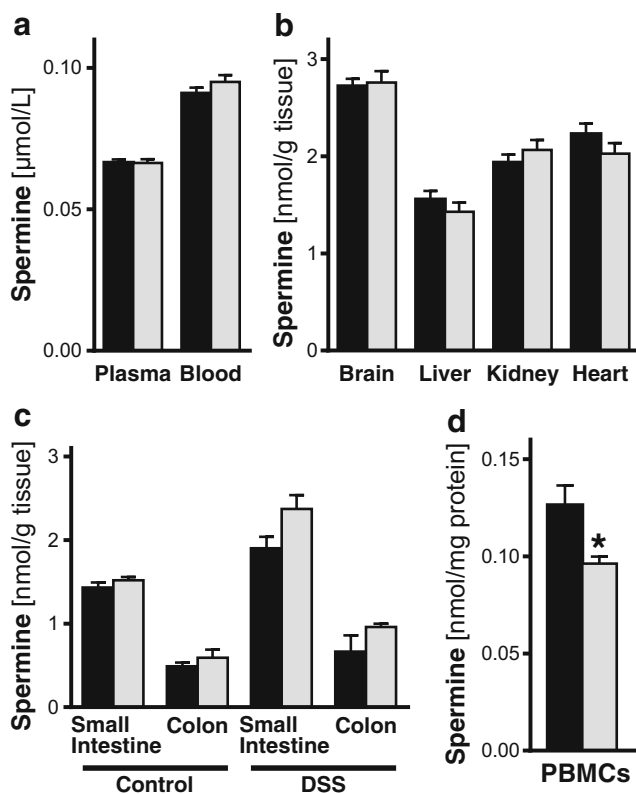
Fig. 4 Interaction between spermine and OCTN1. (**a**) HEK293/OCTN1 (closed circles), HEK293/L503F-OCTN1 (closed diamonds), and mock (open circles) cells were incubated with medium containing [^{3}H]spermine (1 nM) and 10% FBS in a humidified incubator at 37°C and 5% CO$_2$. (**b**) Cells were incubated with medium containing various concentrations of [^{3}H]spermine and 10% FBS for 6 h in a humidified incubator at 37°C and 5% CO$_2$. Radioactivity associated with cells after washing with ice-cold buffer was determined. (**c**, **d**) Uptake of [^{3}H]spermine for 2 h (**c**) and [^{14}C]TEA for 1 min (**d**) was measured in the absence or presence of 1 mM verapamil in HEK293/L503F-OCTN1 (closed bars), and mock (open bars) cells. (**e**) Uptake of ERGO-d9 for 5 min in the presence of various concentrations of spermine and 10% FBS was measured in HEK293/L503F-OCTN1 and mock cells. L503F-OCTN1-mediated uptake of ERGO-d9 was then calculated by subtracting the uptake in mock cells from that in HEK293/L503F-OCTN1 cells, and shown. (**f**) Uptake of [^{14}C]TEA for 1 min in the presence of various concentrations of spermine and 10% FBS was measured in HEK293/L503F-OCTN1 and mock cells. L503F-OCTN1-mediated uptake of [^{14}C]TEA was calculated and shown. Each point represents the mean ± S.E.M. ($n = 6$–9). *, $p < 0.05$ compared to the mock; #, $p < 0.05$ compared to WT-OCTN1; [], $p < 0.05$ compared to each control.

than those in wild-type mice at 3 and 6 h, and 1, 3, and 6 h, respectively (Fig. 6a, b). Conversely, mRNA expression of *IL-1β* and *IL-6* was similar between two strains (Fig. 6c, d). Spermine concentration in the peritoneal macrophages of *octn1$^{-/-}$* mice tended to be lower than that in wild-type mice (Fig. 6e). Thus, *octn1* gene deletion may partially accelerate recovery from inflammation in macrophages, although direct involvement of spermine in the inflammation was not fully demonstrated, and other OCTN1 substrates may also affect the cytokine induction.

DISCUSSION

In the present study, we identified spermine as a putative endogenous OCTN1 substrate using a novel approach that

combined both transporter- and structure-selective metabolomics (Fig. 1). With this method, endogenous OCTN1 substrates in colon tissues of DSS-induced colitis mice were taken up into HEK293/OCTN1 cells, their amino groups were derivatized with APDS, and selectively detected by precursor ion scanning targeted to the APDS moiety (Fig. 1). Indeed, spermine was identified by this method and its concentration in PBMCs was regulated at least partially by OCTN1 (Fig. 5). This combination metabolomics approach may be useful for the identification of endogenous OCTN1 substrates in inflamed organs. Transporter-selective metabolomics (Fig. 1a) alone has already been applied in the identification of several transporter substrates (9,29–32); however, this approach can report false-positive differences between transporter-expressing and control cells because heterologous transfection of transporter genes may induce up- or down-regulation of

Fig. 5 Effects of *OCTN1* gene deletion on endogenous spermine concentrations in blood and tissues in mice. (**a**, **b**) Spermine concentrations in plasma, blood, and tissues measured in wild type (black bars) and *octn1*$^{-/-}$ (gray bars) mice. (**c**) Spermine concentrations measured in epithelial cells obtained from small intestines and colons of DSS-induced colitis or control mice. (**d**) Spermine concentrations in PBMCs that were isolated from the blood of wild type (black bars) and *octn1*$^{-/-}$ (gray bars) mice using density-gradient centrifugation. Each value represents the mean ± S.E.M. (n = 6, 3–6, and 9 in panels **a**-**b**, **c**, and **d**, respectively). *, Significant difference compared to wild-type mice ($p < 0.05$).

other endogenous proteins and result in nonspecific changes in the amounts of endogenous compounds in transporter-expressing cell lines. Therefore, the additional structure-selective metabolomics step of APDS derivatization of amino groups (Fig. 1b) was included in the present study to further select for transporter substrates. This second step alone may also limit OCTN1 substrate selection; for example, APDS reacts with only primary and secondary amines, whereas OCTN1 can accept quaternary amines like ERGO. For further identification of novel OCTN1 substrates, therefore, establishing other derivatizing reagents that can more specifically react with OCTN1 substrates will be needed.
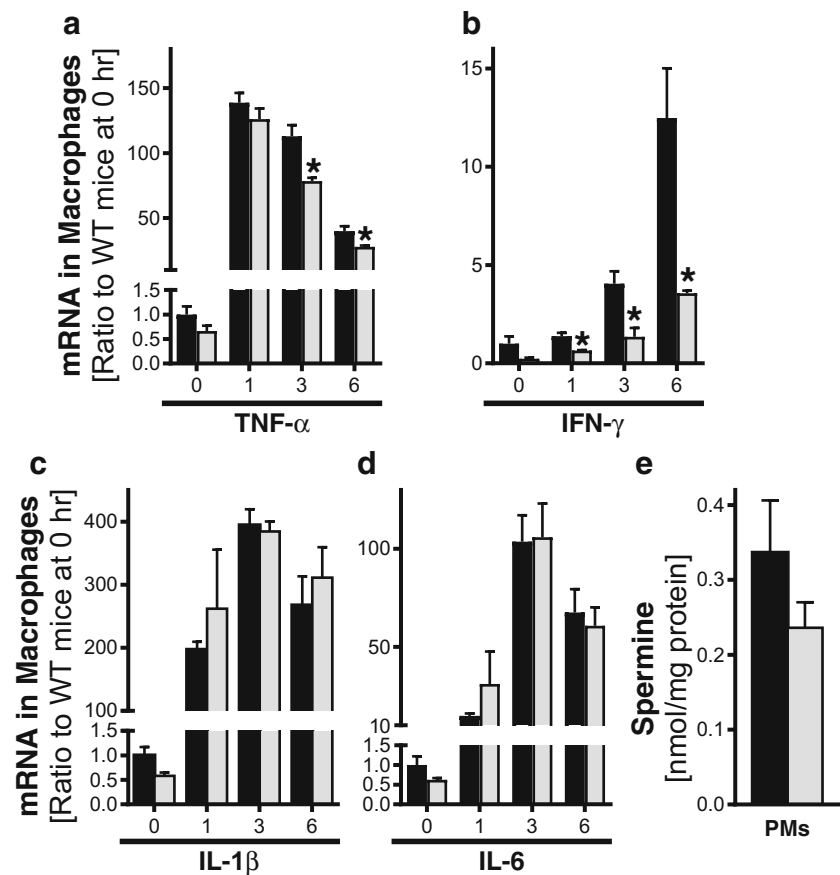
The *octn1*$^{-/-}$ mice have slight phenotypic differences from wild-type mice under normal breeding conditions, but exhibit severe inducible phenotypes including DSS-induced colitis (19), ischemic reperfusion of the small intestines (24), liver fibrosis (21), and chronic kidney disease (33). Since OCTN1 is a poly-specific transporter, such inducible phenotypes in *octn1*$^{-/-}$ suggest that a certain endogenous OCTN1

substrate(s) could play a role in disease-associated conditions. To identify such endogenous substrates, extracts from diseased colon tissues were used as a substrate source to treat HEK293/OCTN1 cells and used concentrate OCTN1 substrate compounds for analysis (Fig. 1a). An approach using similar biological samples has already been used to identify endogenous substrates of several transporters including OCTN1; ERGO was originally identified as an OCTN1 substrate by performing uptake metabolomics studies in OCTN1-expressing cells with human plasma as a substrate source (9). Urine and bile fluids were also utilized as substrate sources in transporter-expressing vesicles to identify endogenous substrates of ABCC2 and ABCG2, respectively (29,31). These previous approaches, however, utilized fluid biological samples obtained from healthy humans or animals, but not those in diseased states. Thus, as shown in the present study, extracts from diseased tissue samples are a promising source for the identification of transporter endogenous substrates; although one limitation of this approach is that the tissue extracts may exclude certain compounds that are disease-specific transporter substrates during the extraction process. For example, since the colon tissue extracts were obtained after removing lipids and proteins by adding organic solvents, such molecules were excluded from the metabolomics approach in the present study.

In Fig. 2j, unlabelled spermine was measured by LC-MS/MS after derivatization, whereas radioisotope-labelled spermine was used in Fig. 4a, b. Thus, the amount of spermine detected in Fig. 2j could be the sum of that newly taken up during the uptake experiment and that originally present in the cells before start of the uptake experiment. Therefore, OCTN1-mediated uptake of spermine can occur during the cell culture before the start of the uptake experiment in Fig. 2j, and this might be advantageous to detect the higher uptake of spermine in HEK293/WT-OCTN1 compared with mock cells (Fig. 2j). Similar phenomenon was previously reported in the uptake of thiamine, which is component of culture medium, by OCT1 during the cell culture (32). However, it should be noted that the amount of unlabeled spermine (Fig. 2j) may also be affected by the uptake of precursors of spermine, which include ornithine, putrescine, and spermidine. Although the present metabolomics analysis did not identify any of these precursors, their possible transport by OCTN1 needs to be clarified by further analyses. On the other hand, spermine detected in Fig. 4a, b could only represent that newly taken up during the uptake experiment, and significantly higher uptake of spermine in HEK293/L503F-OCTN1 cells, but not in WT-OCTN1 cells, compared with mock cells was observed (Fig. 4a). Since L503F-OCTN1 shows relatively higher uptake of spermine compared with WT-OCTN1 (Fig. 4a), such significantly higher uptake in HEK293/L503F-OCTN1 of spermine than mock cells could be observed even in relatively short period.

Fig. 6 Effects of *OCTN1* gene deletion on LPS-induced inflammation and spermine concentration in isolated peritoneal macrophages. Peritoneal macrophages (PMs) were isolated from wild-type (black bars) and *octn1*$^{-/-}$ (gray bars) mice and cultured for 24 h to remove non-attached cells. PMs were stimulated by LPS (100 ng/mL), and mRNA expression of (**a**) *Tnf-α*, (**b**) *Ifn-γ*, (**c**) *Il-1β*, and (**d**) *Il-6* were measured. Data were normalized by *Gapdh* gene expression. In panel (**e**), spermine concentration in PMs cultured for 24 h is presented. Each value represents the mean ± SEM (*n* = 3). The asterisk (*) indicates *p* < 0.05 compared to wild-type mice.

Spermine concentration in colonic epithelial cells (CECs) of patients with IBD was previously reported to be lower than that in control groups (34), probably because of an increase in spermine metabolism by spermine oxidase during IBD (35). It should be noted that the OCTN1 variant L503F exhibited higher uptake of [^{3}H]spermine compared to wild-type OCTN1 (Fig. 4), and this variant is associated with an increased susceptibility in Crohn's disease (6,7). Spermine is mainly metabolized by spermine oxidase, and, the toxic amino aldehyde acrolein, is produced during the oxidation (28). The higher spermine uptake by L503F-OCTN1 might thus provoke spermine metabolism and acrolein-induced toxicity in the cells, and this may partially explain the higher risk of inflammation in L503F-OCTN1 variant possessing patients. This hypothesis that OCTN1-mediated spermine uptake partially induces inflammation, was supported by the higher spermine concentration in PBMCs (Fig. 5d) and higher mRNA levels of several inflammatory cytokine genes in peritoneal macrophage cells isolated from wild-type mice compared with those isolated from *octn1*$^{-/-}$ mice (Fig. 6). Further studies will be needed to clarify the role of OCTN1-mediated spermine uptake in the development of IBD.

Limited information is available about spermine transporters in mammals. Human SLC18B1 (36) and rat Slc22a1 (37) were identified as spermine transporters *in vitro*, although contribution of these transporters to spermine homeostasis *in vivo* is still unknown. Spermine intracellularly synthesized is rapidly catabolized (28). Most of spermine in mammalian cells was bound to RNA (65–85%), and only 2–5% of spermine exists in its free form (38). Such small available fractions in the cytosol may hinder the exact estimation of the contribution of transporters, including OCTN1, in spermine disposition *in vivo*. Therefore, while little difference in spermine concentrations in PBMCs and peritoneal macrophages was observed between wild-type and *octn1*$^{-/-}$ mice (Figs. 5d, 6e), this does not necessarily mean OCTN1 is not a significant contributor to spermine concentration in inflammatory cells. In addition, putrescine, which like spermine, is in the polyamine family, was previously assumed to be an endogenous substrate of OCTN1 and associated with the high risk of Crohn's disease in the L503F-OCTN1 variant (6), although OCTN1-mediated transport of putrescine has not yet been directly demonstrated.

One of the beneficial features of the derivatization of amino groups with APDS (Fig. 1b) is the detection of compounds that are difficult to directly detect by LC-MS(/MS). OCTN1 preferentially recognizes hydrophilic compounds as substrates, and such compounds are not easily retained in conventional reverse-phase chromatography (16). On the other hand, derivatization with APDS increases lipophilicity of these compounds, and they can be separated by reverse-phase

chromatography, which improves detection with higher sensitivity in mass spectrometry (22). In fact, it is difficult to measure spermine concentration using conventional reverse phase chromatography because it easily absorbs into the column resin (39); whereas, spermine derivatized with APDS enabled us to directly measure its concentration in plasma and tissues (Fig. 5). Furthermore, our results are consistent with a recent report of the detection of spermine in human plasma by the same derivatization (40). Moreover, the derivatization reaction may be useful to estimate the number of functional groups in unknown chemical structures from MS spectra (Fig. 3c). This information could help identify compounds in untargeted metabolomics; for example, our present study has clarified the conjugation of four APDS fragments in m/z 683.3734, suggesting the target compound includes four free amino groups. The use of another type of structure-selective metabolomics has identified endogenous substrates of ABCC2, ABCG2, and ABCC3 using neutral loss scanning to selectively detect compounds conjugated with glucuronic acid and/or sulfate (29–31). Glucuronides and sulfate moieties are easily released from their conjugated compounds during collision-induced dissociation, and this approach would be useful to detect compounds containing the same chemical moieties by neutral loss scanning since no further derivatization method is necessary to detect them, although this other approach can be applied only to conjugated compounds.

In conclusion, our use of a combination metabolomics approach (Fig. 1) would be useful to identify spermine as an endogenous substrate of OCTN1. This finding suggests a possible role for OCTN1-mediated uptake of spermine during intestinal inflammation.

ACKNOWLEDGMENTS AND DISCLOSURES

REFERENCES

1. Lin L, Yee SW, Kim RB, Giacomini KM. SLC transporters as therapeutic targets: emerging opportunities. Nat Rev Drug Discov. 2015;14(8):543–60.

2. Rioux JD, Silverberg MS, Daly MJ, Steinhart AH, McLeod RS, Griffiths AM, et al. Genomewide search in Canadian families with inflammatory bowel disease reveals two novel susceptibility loci. Am J Hum Genet. 2000;66(6):1863–70.

3. Tokuhiro S, Yamada R, Chang X, Suzuki A, Kochi Y, Sawada T, et al. An intronic SNP in a RUNX1 binding site of SLC22A4, encoding an organic cation transporter, is associated with rheumatoid arthritis. Nat Genet. 2003;35(4):341–8.

4. Hou X, Mao J, Li Y, Li J, Wang W, Fan C, et al. Association of single nucleotide polymorphism rs3792876 in SLC22A4 gene with autoimmune thyroid disease in a Chinese Han population. BMC Med Genet. 2015;16:76.

5. Santiago JL, Martinez A, de la Calle H, Fernandez-Arquero M, Figueredo MA, de la Concha EG, et al. Evidence for the association of the SLC22A4 and SLC22A5 genes with type 1 diabetes: a case control study. BMC Med Genet. 2006;7:54.

6. Peltekova VD, Wintle RF, Rubin LA, Amos CI, Huang Q, Gu X, et al. Functional variants of OCTN cation transporter genes are associated with Crohn disease. Nat Genet. 2004;36(5):471–5.

7. Xuan C, Zhang BB, Yang T, Deng KF, Li M, Tian RJ. Association between OCTN1/2 gene polymorphisms (1672C-T, 207G-C) and susceptibility of Crohn's disease: a meta-analysis. Int J Color Dis. 2012;27(1):11–9.

8. Tamai I, Yabuuchi H, Nezu J, Sai Y, Oku A, Shimane M, et al. Cloning and characterization of a novel human pH-dependent organic cation transporter, OCTN1. FEBS Lett. 1997;419(1):107–11.

9. Grundemann D, Harlfinger S, Golz S, Geerts A, Lazar A, Berkels R, et al. Discovery of the ergothioneine transporter. Proc Natl Acad Sci U S A. 2005;102(14):5256–61.

10. Grigat S, Harlfinger S, Pal S, Striebinger R, Golz S, Geerts A, et al. Probing the substrate specificity of the ergothioneine transporter with methimazole, hercynine, and organic cations. Biochem Pharmacol. 2007;74(2):309–16.

11. Pochini L, Scalise M, Galluccio M, Pani G, Siminovitch KA, Indiveri C. The human OCTN1 (SLC22A4) reconstituted in liposomes catalyzes acetylcholine transport which is defective in the mutant L503F associated to the Crohn's disease. Biochim Biophys Acta. 2012;1818(3):559–65.

12. Drenberg CD, Gibson AA, Pounds SB, Shi L, Rhinehart DP, Li L, et al. OCTN1 is a high-affinity carrier of nucleoside analogues. Cancer Res. 2017;77(8):2102–11.

13. Taubert D, Grimberg G, Jung N, Rubbert A, Schomig E. Functional role of the 503F variant of the organic cation transporter OCTN1 in Crohn's disease. Gut. 2005;54(10):1505–6.

14. Taubert D, Jung N, Goeser T, Schomig E. Increased ergothioneine tissue concentrations in carriers of the Crohn's disease risk-associated 503F variant of the organic cation transporter OCTN1. Gut. 2009;58(2):312–4.

15. Urban TJ, Yang C, Lagpacan LL, Brown C, Castro RA, Taylor TR, et al. Functional effects of protein sequence polymorphisms in the organic cation/ergothioneine transporter OCTN1 (SLC22A4). Pharmacogenet Genomics. 2007;17(9):773–82.

16. Futatsugi A, Masuo Y, Kawabata S, Nakamichi N, Kato Y. L503F variant of carnitine/organic cation transporter 1 efficiently transports metformin and other biguanides. J Pharm Pharmacol. 2016;68(9):1160–9.

17. Urban TJ, Brown C, Castro RA, Shah N, Mercer R, Huang Y, et al. Effects of genetic variation in the novel organic cation transporter, OCTN1, on the renal clearance of gabapentin. Clin Pharmacol Ther. 2008;83(3):416–21.

18. Cheah IK, Halliwell B. Ergothioneine; antioxidant potential, physiological function and role in disease. Biochim Biophys Acta. 2012;1822(5):784–93.

19. Shimizu T, Masuo Y, Takahashi S, Nakamichi N, Kato Y. Organic cation transporter Octn1-mediated uptake of food-derived antioxidant ergothioneine into infiltrating macrophages during intestinal

inflammation in mice. Drug Metab Pharmacokinet. 2015;30(3): 231–9.

20. Maeda T, Hirayama M, Kobayashi D, Miyazawa K, Tamai I. Mechanism of the regulation of organic cation/carnitine transporter 1 (SLC22A4) by rheumatoid arthritis-associated transcriptional factor RUNX1 and inflammatory cytokines. Drug Metab Dispos. 2007;35(3):394–401.

21. Tang Y, Masuo Y, Sakai Y, Wakayama T, Sugiura T, Harada R, *et al.* Localization of xenobiotic transporter OCTN1/SLC22A4 in hepatic stellate cells and its protective role in liver fibrosis. J Pharm Sci. 2016;105(5):1779–89.

22. Shimbo K, Oonuki T, Yahashi A, Hirayama K, Miyano H. Precolumn derivatization reagents for high-speed analysis of amines and amino acids in biological fluid using liquid chromatography/electrospray ionization tandem mass spectrometry. Rapid Commun Mass Spectrom. 2009;23(10):1483–92.

23. Kato Y, Kubo Y, Iwata D, Kato S, Sudo T, Sugiura T, *et al.* Gene knockout and metabolome analysis of carnitine/organic cation transporter OCTN1. Pharm Res. 2010;27(5):832–40.

24. Ishimoto T, Nakamichi N, Hosotani H, Masuo Y, Sugiura T, Kato Y. Organic cation transporter-mediated ergothioneine uptake in mouse neural progenitor cells suppresses proliferation and promotes differentiation into neurons. PLoS One. 2014;9(2):e89434.

25. Tanaka S, Fujita Y, Parry HE, Yoshizawa AC, Morimoto K, Murase M, *et al.* Mass++: a visualization and analysis tool for mass spectrometry. J Proteome Res. 2014;13:3846–53.

26. Zhang X, Goncalves R, Mosser DM. The isolation and characterization of murine macrophages. Curr Protoc Immunol. 2008;Chapter 14:Unit 14 1.

27. Yabuuchi H, Tamai I, Nezu J, Sakamoto K, Oku A, Shimane M, *et al.* Novel membrane transporter OCTN1 mediates multispecific, bidirectional, and pH-dependent transport of organic cations. J Pharmacol Exp Ther. 1999;289(2):768–73.

28. Igarashi K, Kashiwagi K. Modulation of cellular function by polyamines. Int J Biochem Cell Biol. 2010;42(1):39–51.

29. Krumpochova P, Sapthu S, Brouwers JF, de Haas M, de Vos R, Borst P, *et al.* Transportomics: screening for substrates of ABC transporters in body fluids using vesicular transport assays. FASEB J. 2012;26(2):738–47.

30. van de Wetering K, Feddema W, Helms JB, Brouwers JF, Borst P. Targeted metabolomics identifies glucuronides of dietary phytoestrogens as a major class of MRP3 substrates in vivo. Gastroenterology. 2009;137(5):1725–35.

31. van de Wetering K, Sapthu S. ABCG2 functions as a general phytoestrogen sulfate transporter in vivo. FASEB J. 2012;26(10):4014–24.

32. Chen L, Shu Y, Liang X, Chen EC, Yee SW, Zur AA, *et al.* OCT1 is a high-capacity thiamine transporter that regulates hepatic steatosis and is a target of metformin. Proc Natl Acad Sci U S A. 2014;111(27):9983–8.

33. Shinozaki Y, Furuichi K, Toyama T, Kitajima S, Hara A, Iwata Y, *et al.* Impairment of the carnitine/organic cation transporter 1-ergothioneine axis is mediated by intestinal transporter dysfunction in chronic kidney disease. Kidney Int. 2017;92(6):1356–69.

34. Weiss TS, Herfarth H, Obermeier F, Ouart J, Vogl D, Scholmerich J, *et al.* Intracellular polyamine levels of intestinal epithelial cells in inflammatory bowel disease. Inflamm Bowel Dis. 2004;10(5):529–35.

35. Hong SK, Chaturvedi R, Piazuelo MB, Coburn LA, Williams CS, Delgado AG, *et al.* Increased expression and cellular localization of spermine oxidase in ulcerative colitis and relationship to disease activity. Inflamm Bowel Dis. 2010;16(9):1557–66.

36. Hiasa M, Miyaji T, Haruna Y, Takeuchi T, Harada Y, Moriyama S, *et al.* Identification of a mammalian vesicular polyamine transporter. Sci Rep. 2014;4:6836.

37. Busch AE, Quester S, Ulzheimer JC, Waldegger S, Gorboulev V, Arndt P, *et al.* Electrogenic properties and substrate specificity of the polyspecific rat cation transporter rOCT1. J Biol Chem. 1996;271(51):32599–604.

38. Watanabe S, Kusama-Eguchi K, Kobayashi H, Igarashi K. Estimation of polyamine binding to macromolecules and ATP in bovine lymphocytes and rat liver. J Biol Chem. 1991;266(31): 20803–9.

39. Takayama T, Tsutsui H, Shimizu I, Toyama T, Yoshimoto N, Endo Y, *et al.* Diagnostic approach to breast cancer patients based on target metabolomics in saliva by liquid chromatography with tandem mass spectrometry. Clin Chim Acta. 2016;452:18–26.

40. Arashida N, Nishimoto R, Harada M, Shimbo K, Yamada N. Highly sensitive quantification for human plasma-targeted metabolomics using an amine derivatization reagent. Anal Chim Acta. 2017;954:77–87.